Atmos. Chem. Phys. Discuss., 14, 3875–3915, 2014
www.atmos-chem-phys-discuss.net/14/3875/2014/
doi:10.5194/acpd-14-3875-2014

Atmospheric Chemistry and Physics Discussions

Ambient measurements of biological aerosol particles near Killarney, Ireland: a comparison between real-time fluorescence and microscopy techniques

D. A. Healy[1,*], **J. A. Huffman**[2,3], **D. J. O'Connor**[1], **C. Pöhlker**[3], **U. Pöschl**[3], **and J. R. Sodeau**[1]

[1]University College Cork, Department of Chemistry and Environmental Research Institute, Cork, Ireland
[2]University of Denver, Department of Chemistry and Biochemistry, Denver, Colorado, USA
[3]Max Planck Institute for Chemistry, Multiphase Chemistry and Biogeochemistry Departments, Mainz, Germany
[*]now at: Pepsico, Global Quality Services, Cork, Ireland

Received: 19 January 2014 – Accepted: 28 January 2014 – Published: 11 February 2014

Correspondence to: D. A. Healy (d.healy@ucc.ie) and J. A. Huffman (alex.huffman@du.edu)

Published by Copernicus Publications on behalf of the European Geosciences Union.

Abstract

Primary biological aerosol particles (PBAP) can contribute significantly to the coarse particle burden in many environments, may thus influence climate and precipitation systems as cloud nuclei, and can spread disease to humans, animals, and plants. Measurements of PBAP in natural environments taken at high time- and size- resolution are, however, sparse and so large uncertainties remain in the role that biological particles play in the Earth system. In this study two commercial real-time fluorescence particle sensors and a Sporewatch single-stage particle impactor were operated continuously from 2 August to 2 September 2010 at a rural sampling location in Killarney National Park in south western Ireland. A cascade impactor was operated periodically to collect size-resolved particles during exemplary periods. Here we report the first ambient comparison of the waveband integrated bioaerosol sensor (WIBS-4) with the ultraviolet aerodynamic particle sizer (UV-APS) and also compare these real-time fluorescence techniques with results of fluorescence and optical microscopy of impacted samples. Both real-time instruments showed qualitatively similar behaviour, with increased fluorescent bioparticle concentrations at night when relative humidity was highest and temperature was lowest.

The fluorescent particle number from the FL3 channel of the WIBS-4 and from the UV-APS were strongly correlated and dominated by a 3 µm mode in the particle size distribution. The WIBS FL2 channel exhibited particle modes at approx. 1 and 3 µm, and each were correlated with the concentration of fungal spores commonly observed in air samples collected at the site (ascospores, basidiospores, *Ganoderma* spp.). The WIBS FL1 channel exhibited variable multi-modal distributions turning into a broad featureless single mode after averaging and exhibited poor correlation with fungal spore concentrations, which may be due to the detection of bacterial and non-biological fluorescent particles. *Cladosporium* spp., which are among the most abundant fungal spores in many terrestrial environments, were not correlated with any of the real-time

ACPD
14, 3875–3915, 2014

fluorescence channels, suggesting that the real-time fluorescence instruments are insensitive to PBAP classes with dark, highly absorptive cell walls.

Fluorescence microscopy images of cascade impactor plates showed large numbers of coarse mode particles consistent with the morphology and weak fluorescence expected of sea salt. Some of these particles were attached to biological cells, suggesting that a marine source influenced the PBAP observed at the site and that the ocean may be an important contributor to PBAP loadings in coastal environments.

1 Introduction

The in situ monitoring of primary biological aerosol particles (PBAPs) with high time resolution represents an important technological development made capable, in part, by long-standing, military-led research into the detection of biological warfare agents. The more recent drive to monitor ambient, atmospheric PBAPs is largely related to adverse effects they play in human and agricultural health (e.g. allergic rhinitis, food crop damage) (Shiraiwa et al., 2012; Pöschl, 2005; Lacey and Dutkiewicz, 1994; Patel and Bush, 2000). Several classes of bioaerosols have been shown to act as cloud and ice nuclei in laboratory settings (e.g. Haga et al., 2013; Pummer et al., 2012; Morris et al., 2004, 2013; Diehl et al., 2001; Maki et al., 1974; Möhler et al., 2007), and ambient measurements have shown PBAP to be ubiquitously associated with rain and snowfall as well as present in clouds (Christner et al., 2008; Pöschl et al., 2010; Prenni et al., 2013; DeLeon-Rodriguez et al., 2013; Huffman et al., 2013). Thus, it has been suggested that PBAP may impact precipitation and the hydrological cycle, and may ultimately affect the weather and climate of a region (Morris et al., 2008, 2014; Sands et al., 1982). A review of biological aerosol properties and detection methods is beyond the scope of this text, but comprehensive PBAP overviews are available (e.g. Després et al., 2012; Caruana, 2011; Womack et al., 2010; Madelin, 1994; Ho, 2002; Xu et al., 2011; Fröhlich-Nowoisky et al., 2012, 2009).

ACPD
14, 3875–3915, 2014

Common usage of the term PBAP includes various classes of biological particles, including: viruses; bacteria; fungal, moss and fern spores; pollen; algal and plant cells; insects, mites, and their fragments including excreta (Després et al., 2012). Such PBAPs have been well studied within the aerobiology community for many decades using traditional methods of impact collection followed by microscopic counting and identification procedures. These analyses can be time consuming and require significant processing cost and skill. In contrast, relatively few studies have reported ambient collection and analysis of bioaerosols at high time resolution (e.g. seconds to minutes), due to the lack of instrumentation capable of monitoring particles on such fast timescales. Recent studies utilizing real-time PBAP measurements have collected and analysed ambient PBAP data for periods as long as 18 consecutive months (Schumacher et al., 2013; Toprak and Schnaiter, 2013; Pan et al., 2007; Gabey et al., 2011; Huffman et al., 2010). Such measurements obtained with high-time resolution can subsequently aid our understanding of atmospheric PBAP properties including sub-diurnal boundary layer transport and cloud formation. Recently work to model bioaerosol emissions on global and regional scales have attempted to quantify the impact that PBAP have on coarse aerosol loadings and IN properties (Hummel et al., 2014; Hoose et al., 2010, 2009b; e.g. Burrows et al., 2009a; Sesartic et al., 2013; Heald and Spracklen, 2009), however more detailed understanding of PBAP inputs are necessary to constrain model results.

A number of optical systems utilizing light/laser-induced fluorescence (LIF) have been developed to detect airborne biological material based on the presence of biological fluorophores in the particle. Instrumentation available for military research use but not commercial/civilian use include: the Aerosol Fluorescence Spectrum Analyser (AFSA) (Pinnick et al., 1995, 2004; Pan et al., 2011) and the Single Particle Fluorescence Analyser (SPFA) (Eversole et al., 1999; Sivaprakasam et al., 2011). Within approximately the last decade, commercially available devices have become obtainable for purchase and use by non-military communities. Similar to approaches developed in military-based laboratories, these commercial instruments provide real-time (on-line)

ACPD
14, 3875–3915, 2014

detection of biological particles suspended in the air. Two single particle fluorescence instruments that have been used most widely within the atmospheric aerosol research community include the ultraviolet aerodynamic particle sizer (UV-APS; TSI, Inc. model 3314, St. Paul, MN) (Huffman et al., 2010; Hairston et al., 1997; Brosseau et al., 2000) and the waveband integrated bioaerosol sensor (WIBS; originally developed by the University of Hertfordshire, UK and now licensed and sold by Droplet Measurement Technology, Boulder, CO) (Stanley et al., 2011; Foot et al., 2008; Kaye et al., 2005). Fluorescent emission excited by ~ 360 nm radiation is considered to include the presence of metabolites (e.g. NAD(P)H, riboflavin) within living cells. Emission related excited by ~ 280 nm radiation is usually attributed to proteins and amino acids present in all biological material, whether living or dead (Pöhlker et al., 2012, 2013). However observed fluorescence signals at a given wavelength are likely to arise from a complex mixture of bio-fluorophores in the particle (Pöhlker et al., 2012).

A growing body of published reports suggest that particle autofluorescence can be used, to a first approximation, to separately detect biological and non-biological particles (Robinson et al., 2013; Pöhlker et al., 2012; Huffman et al., 2012). However, secondary organic aerosol (SOA), humic-like substance (HULIS), and other atmospheric particles have been suggested to interfere with detection of ambient biological particles via fluorescence (e.g. Huffman et al., 2010; Gabey et al., 2013; Lee et al., 2013; Pöhlker et al., 2012). Measurements in the remote Amazon basin of Brazil showed that fluorescent particle number closely approximated biological particles measured by electron microscopy (Huffman et al., 2012), suggesting that techniques utilizing particle autofluorescence can be used in some geographic environments as first-approximation classifiers between biological and non-biological particles and can provide a lower limit for the atmospheric abundance of PBAP in the super-micron (> 1 µm) size range. However, more work is needed to better understand the scenarios in which this assumption holds.

This study represents the first co-located ambient deployment of the UV-APS and WIBS-4 instruments. Results suggest a good qualitative comparison between the two

ACPD
14, 3875–3915, 2014

real-time techniques as well as with optical microscopy measurements performed on samples simultaneously collected via impaction. The comparisons reported here help characterize real-time fluorescence instrument capabilities for atmospheric bioaerosol measurement and will improve the ability of the atmospheric research community to reliably detect PBAP.

2 Methodology

2.1 Location of sampling site

Sampling was performed between 2 August and 2 September 2010 within Killarney National Park (KNP), Kerry, which is situated in south-west Ireland (N 52°01.263′ W 09°30.553′). The site was located on the eastern perimeter of Reenadinna Woods, in a small clearing (~ 30 m × 50 m) of manicured grass surrounded by *Taxus baccata*, Yew trees and within meters of Muckross Lake (online Supplement, Fig. S1). KNP is one of the western-most European national parks. The site can be characterized as clean and rural, with local south-westerly winds and incoming air masses influenced most heavily from pristine Atlantic trajectories, including minimal influence from anthropogenic emissions. The site comprises mixed deciduous trees and rich undergrowth. A list of typical botanic species found in Reenadinna Woods is outlined elsewhere (Kelly, 1981).

All instruments were housed in a purpose-built mobile laboratory trailer (3 m length) which was positioned immediately adjacent to a lawn area in front (~ 5 m) of the unoccupied Arthur Vincent House from where electrical power was obtained. Sample inlets extended vertically from the mobile laboratory were approximately 2.5–3.0 m in height a.g.l. and positioned approximately 4 m from the nearest trees.

ACPD
14, 3875–3915, 2014

2.2 Instrumentation

2.2.1 WIBS

The waveband integrated bioaerosol sensor Model 4 is a prototype of a series of real-time biological particle sensors developed by the University of Hertfordshire in the UK (Stanley et al., 2011; Foot et al., 2008; Kaye et al., 2005; Gabey et al., 2011; Healy et al., 2012a, b; O'Connor et al., 2013). Briefly, the WIBS-4 consists of a central optical chamber, around which are arranged: (i) a continuous-wave 635 nm diode laser used for the initial detection of particles and the determination of particle size (optical diameter); (ii) a forward light-scattering quadrant photomultiplier used in the determination of particle size and asymmetry; and (iii) two pulsed xenon flashtube UV sources emitting sequentially at 280 nm and 370 nm. Fluorescence emission is detected in two bands: 310–400 nm (band 1) and 420–650 nm (band 2). Thus, for each particle, three fluorescence measurements are provided: (i) excitation at 280 nm, emission in band 1 (FL1); (ii) excitation at 280 nm, emission in band 2 (FL2); and (iii) excitation at 370 nm, emission in band 2 (FL3). For each individual particle detected, the instrument also provides the optical particle size (D_o) and the particle asymmetry factor (A_f), which is a parameter that describes the degree of symmetry for the forward scattered light (Kaye et al., 2005). Light detected by a four-quadrant PMT are combined to calculate an A_f; a spherical particle would have A_f of 0, and rod-shaped fibres would yield A_f near 100 (Gabey et al., 2010).

The particle counting efficiency of the WIBS-4 used in the current study drops below unity at $D_o < 0.69$ µm with D_{50} at 0.49 µm (Healy et al., 2012b). Therefore, number concentrations for particles with $D_o < 0.69$ µm should be considered as lower limit values. The upper size limit is defined as a function of the PMT gain setting and was approx. 13 µm for this study. It is possible to operate the Hertfordshire WIBS-4 instruments at a different gain setting for the detection of particles up to approximately 31 µm in diameter. However, the configuration utilized here only permits optical particle sizing of particles between approx. 0.5 and 13 µm.

ACPD
14, 3875–3915, 2014

The trigger threshold setting of WIBS-4 (Trig) is an instrumental parameter that can be adjusted to predefine the lower particle size limit for which the firing of the xenon UV flash lamps (i.e. fluorescence excitation) will be triggered. The effects of such adjustments, i.e. minimum particle size as a function of Trig setting, had not previously been explored in an ambient setting. Furthermore WIBS instruments manufactured by the University of Hertfordshire are each unique prototypes and therefore the operational settings are not necessarily comparable between instruments. Three Trig settings were used for the WIBS-4 during the campaign (see also Sect. 3.2). A Trig setting of 8 (2–5 August) corresponded to minimum detectable particle size of 0.52 µm (channel ≥ 1; see Table S1). A Trig setting of 20 (5–18 and 27–31 August) corresponded to a minimum particle size of 0.65 µm (channel ≥ 4). Lastly, a Trig setting of 30 (23–27 August and 31 August–2 September) corresponded to a minimum particle size of 0.75 µm (channel ≥ 6).

The performance of the two Xe flashtubes within the WIBS-4 was monitored throughout the measurement period. Flashtube power output values were recorded; upper and lower limit values were determined as $\pm 3\sigma$ (as standard deviation) from the mean. All particles resulting from UV flashes with power outside these bounds were eliminated from the fluorescent particle number concentration calculations. Note, however, that the total particle concentrations remained unaffected.

2.2.2 UV-APS

An ultraviolet aerodynamic particle sizer was utilized and operated using standard procedures (e.g. Huffman et al., 2010) and thereby provided 5 min ensemble averages of number concentration, fluorescence intensity, and size of particles (Hairston et al., 1997; Brosseau et al., 2000). Aerodynamic particle sizing (D_a) in the diameter range between 0.5 and 20 µm is obtained by measuring time of particle flight between two red (633 nm) He-Ne interrogating lasers. Optical excitation of the individual particles is provided by a pulsed Nd:YAG laser operating at 355 nm. Subsequent fluorescence is collected in a single bin (not wavelength dispersed) within the wavelength range

ACPD
14, 3875–3915, 2014

between 420 and 575 nm. UV-APS particle transmission drops below unity at approximately 0.8 µm, with D_{50} approx. 0.54 µm (Huffman et al., 2012), and thus particles smaller than approximately 1 µm are conservatively treated as lower limit values.

2.2.3 Real-time fluorescence instrument comparison

Both WIBS-4 and UV-APS instruments sampled ambient air from the same inlet as shown in Fig. S2. The vertical inlet line consisted of 0.5 inch stainless steel tube and was connected to a 0.5 inch Y-splitter with Swagelok fittings. Connections to both instruments after the split were made using conductive rubber tubing with an internal diameter of approx. 0.75 inch (Simolex Rubber Corp., Plymouth, MI). A by-pass flow of 2.4 L min^{-1} was drawn through a Swagelok tee (at 90°) from the WIBS-4 line to match flows at 4.8 L min^{-1} on either branch of the Y-junction. Flow rates were regularly checked throughout the sample line with an external flowmeter (TSI Inc. Model 4140 Thermal Mass Flowmeter). The instruments and auxiliary pump pulled a total flow of 9.6 L min^{-1} through the inlet.

The WIBS-4 records the size of each individual particle sampled, but particles were binned according to UV-APS particle size channels for ease of comparison. Integrated particle number concentrations for each instrument are given for the size range greater than 1 µm in all cases here. A summary of the characteristic features and settings used by both WIBS-4 and UV-APS as operated here are outlined in Table 1.

The detection limit for each fluorescence channel of the WIBS-4 is defined as the mean fluorescence signal detected during > 10 min. of forced trigger data acquisition mode with no particle flow (i.e. pump off) (Gabey et al., 2010). Hence for each fluorescence channel (FL1, FL2, and FL3) the measured detection limit is taken as the minimum fluorescence intensity that can be reliably obtained by WIBS-4. In contrast the UV-APS bins the fluorescence intensity of individual particles into one of 64 channels. Particles with no measured fluorescence signal appear in channel 1. For the current study particles that give fluorescence signals in channels > 3 were defined as FBAP (Huffman et al., 2010).

ACPD
14, 3875–3915, 2014

WIBS-4 photomultiplier tube (PMT) voltage values were 0.701 V for FL1 and 0.649 V for both FL2 and FL3. The UV-APS PMT voltage was set 380 V as set by the factory to exclude polystyrene latex spheres (PSL) from being characterized as fluorescent. Increasing the UV-APS PMT setting allows for more sensitive detection of particle fluorescence, but also increased the likelihood of weakly fluorescent non-biological particles being counted as FBAP.

2.2.4 Sporewatch particle impactor

The Burkard Sporewatch Sampler (Burkard Scientific, UK) is a volumetric Hirst-type particle trap that operates by drawing air in through an orifice at a constant rate (10 L min^{-1}), allowing particles to impact onto silicone-coated tape (Lanzoi) mounted on a rotating drum (Hirst, 1952). The sampler was mounted on the roof of the mobile laboratory trailer (sampling height ~ 3 m above ground) and operated to rotate at a rate of one revolution per week, with start and end times manually recorded. Tapes were changed weekly, stored in air-sealed bags at ~ 4 °C and then cut into seven daily segments for analysis. Tape segments were mounted on microscope slides and counts of the identifiable fungal spores and pollen species were recorded. Microscope slides were stained with fuchsine (Sigma Aldrich) and the samples were examined under x400 magnification using an optical light microscope (VWR, TR500) according to regulations of the British Aerobiology Federation (Lacey and Venette, 1995). A longitudinal counting method was used, meaning that microscopic observation was performed in one continuous sweep through the centre of the 24 h tape. Only 3 % of the total tape area is observed at a given time by this method and particle concentrations are scaled accordingly. A more detailed description of the method is described elsewhere (Sterling et al., 1999; Lacey and West, 2006). Count values were converted into atmospheric number concentrations by scaling to the full tape width and dividing by the volumetric flow rate of the sampler after assuming that particles were deposited onto the tape with unit efficiency. Resultant concentrations are listed as counts per cubic centimeter of air (cm^{-3}).

ACPD
14, 3875–3915, 2014

Particle counting by this technique is done manually, and so several biases are possible. First, both the sensitivity and selectivity of the characterization is user-dependent. In this case, fungal spores and pollen grains were investigated and counted. Particles smaller than approximately 2 µm were not counted. Individual bacteria or small bacterial agglomerates, for example, would thus not have been counted by this method. Further, many fungal spores are hyaline (translucent) in nature and are therefore difficult to enumerate via optical microscopy. Lastly, the collection efficiency of the Sporewatch impactor drops below unity for particles smaller than approximately 3–5 µm (Khattab and Levetin, 2008). For these reasons, particle concentration values reported here should be taken as lower limit values.

2.2.5 MOUDI particle impactor

Size-resolved particle samples were collected using a micro-orifice uniform deposition impactor (MOUDI; MSP, model 110) at a flow-rate of 30 L min^{-1} via a dedicated inlet. Cut points of aerosol size fractionation have been discussed elsewhere (Marple et al., 1991). Samples were collected onto glass microscope slides for subsequent analysis via fluorescence microscopy.

2.2.6 Fluorescence microscopy

Fluorescence microscopy images were taken using a BZ-9000 Fluorescence Microscope (Keyence, Inc., Osaka, Japan). The instrument was equipped with a super high-compression mercury lamp (120 W) and a 2/3-inch, 1.5 mega pixel monochrome CCD. The following fluorescence filters were used to take images in different spectral ranges: OP-66834 DAPI-BP (λ_{ex} = 360/20 nm, $\lambda_{Dichroic}$ = 400 nm, λ_{Absorp} = 460/25 nm), OP-66836 GFP-BP (λ_{ex} = 470/20 nm, $\lambda_{Dichroic}$ = 495 nm, λ_{Absorp} = 535/25 nm), OP-66838 TexasRed (λ_{ex} = 560/20 nm, $\lambda_{Dichroic}$ = 595 nm, λ_{Absorp} = 630/30 nm). Filter specifications are represented as wavelength and peak width (λ/FWHM).

ACPD
14, 3875–3915, 2014

2.2.7 Meteorological data

Wind speed, wind direction, temperature, humidity, down-welling solar radiation, and rainfall were monitored using a Casella NOMAD weather station mounted on the roof of the mobile laboratory trailer. Measurements were made at 5 min intervals.

3 Results and discussion

3.1 Total particle comparison

The WIBS-4 and UV-APS instruments were operated continuously behind the same inlet for approximately one month. Mean coarse particle number concentration ($N_{T,c}$, $D > 1$ µm) was 32.8 and 32.4 cm^{-3} for WIBS-4 and UV-APS, respectively (Fig. 1), suggesting that there were no significant differences in sampling losses between the two branches of the inlet flow. Figure 1 also shows the correlation of total particle concentration between the instruments, averaged into 5 min samples. The quantitative comparison between the instruments is good, with R^2 value of 0.90 over the campaign. The slope of 0.86, however, suggests that the WIBS method undercounted the total particle concentrations with respect to the UV-APS, especially at concentrations above approx. 50 cm^{-3}. Size-resolved total particle concentrations measured throughout the campaign by both instruments are shown in Fig. S3.

3.2 Overview of fluorescent aerosol trends

A comprehensive overview of biological particle measurements from Spore-watch/optical microscopy, WIBS-4, and UV-APS methods as employed over the whole measurement period is shown in Fig. 2. A coarse view of the measurements shows broad agreement between the techniques, with rhythmic, synchronous increases in particle number across platform and wavelength channel in addition to episodic events of high concentration. Step-functions in the lower size of fluorescent particles from the

ACPD
14, 3875–3915, 2014

FL1 channel (Fig. 2b) highlight periods when different trigger values were used to investigate optimal WIBS-4 operation (Sect. 2.2.1). Ignoring the corresponding fluctuation in lower particle size, as shown by the size-resolved image plots (Fig. 2) and by averaged size distributions from each channel (Fig. 3), the same pattern through time emerges.

The WIBS FL1 channel typically shows a broad, multi-modal distribution, with three distinct modes present for most of 5–18 August, and a bimodal distribution present for most of the rest of the campaign. The presence of the smallest mode (approx. 1.0 µm) during the period when the trigger value was set the lowest highlights the influence that this WIBS setting has on the detection of particles and to the relative shape of fluorescent particle size distributions at small sizes. While discreet modes are present in the time-resolved size distributions (Fig. 2), these fine temporal differences are largely smoothed away when looking at average size distributions over the entire measurement period (Fig. 3a). The WIBS FL2 channel also shows a bimodal distribution, with consistent peaks at approx. 1 and 3 µm in particle size (Figs. 2c and 4b).

The distributions from the WIBS FL3 channel and UV-APS, in contrast, show much stronger signal at the 3 µm particle size and relatively minimal influence from the 1 µm mode. The qualitative correlation in particle size between WIBS FL3 and UV-APS signals is expected, because the excitation wavelengths (370 nm and 355 nm, respectively) are both designed to highlight molecules related to active cellular metabolism (e.g. NAD(P)H and riboflavin) (Eng et al., 1989; Harrison and Chance, 1970; Setlow and Setlow, 1977; Li et al., 1991). While this assumption is a significant oversimplification of the bio-fluorophores present in airborne microorganisms (Pöhlker et al., 2012, 2013), the broad nature of fluorescence excitation and emission spectra along with the relative similarity of excitation wavelength between the two channels leads to the broad consistency. However, despite the relative agreement between the peaks and temporal patterns of WIBS FL3 and UV-APS, Fig. 3c and d show a significantly reduced presence of the 1.2 µm mode in UV-APS compared to the WIBS FL3. This suggests that the UV-APS was less sensitive to smaller fluorescent particles, and thus may not record particles < 2 µm as efficiently as the WIBS-4. The influence of par-

ACPD
14, 3875–3915, 2014

ticle size on fluorescent particle detection is likely a result of the fact that fluorescence detected from individual particles scales as a function of the 2nd to 3rd power of particle diameter, depending on the depth of excitation photon penetration into the interrogated particle (Sivaprakasam et al., 2004; Hill et al., 2001; Tanke et al., 1982). Further, the UV-APS is typically operated with relatively poor sensitivity in order to reduce the possible inclusion of non-biological artefacts in the fluorescence measurement (Huffman et al., 2012).

Both FL1 and FL2 channels are a result of excitation at 280 nm, which can probe proteins, amino acids, and other bio-fluorophores. The differences between FL1 (λ_{em} 310–400 nm) and FL2 (λ_{em} 420–650 nm) channels, however, can highlight different molecules. For example, Pöhlker et al. (2012) show that the FL1 band is much more efficient at detecting certain amino acids and proteins, whereas the FL2 channel detects flavin compounds at higher efficiency. This may also explain the qualitative overlap between the FL2 channel with aspects of each of the FL1 and FL3 channels, while the FL1 and FL3 channels show relatively little similarity in size distribution.

A quantitative comparison between the fluorescence channels detected is provided in Fig. 4, each WIBS channel shown with respect to UV-APS fluorescent particle number. As discussed, of all WIBS channels, FL3 $N_{F,c}$ displays the highest correlation with UV-APS $N_{F,c}$ (R^2 0.78). The correlation between FL2 and UV-APS was also quite high (R^2 0.68), but between FL1 and UV-APS the correlation was poor (R^2 0.34). As mentioned, the good correlation between FL3 and UV-APS is expected, because of the common excitation and emission wavelengths employed by the two measurements. However, the UV-APS undercounts the FL3 measurement by a factor of 2.7 (Fig. 4d). In contrast the WIBS FL1 and FL2 signals result from fundamentally different fluorophores that result in much higher number concentrations.

Results of the Sporewatch analysis show qualitative agreement with temporal cycles from the single particle fluorescence measurements (Fig. 2a); when each of the real-time fluorescence channels peak, a corresponding peak in spore concentrations can be seen as well. A comparison of the diurnal cycles will be discussed in Sect. 3.3. It

ACPD
14, 3875–3915, 2014

is of note that the differing time resolution of the techniques used (5 min for real-time fluorescence instruments, 2 h for Sporewatch) results in small temporal shifts in peaks of number concentrations.

3.3 Real-time fluorescence sensors vs. Sporewatch

The advantage of the Sporewatch technique paired with optical microscopy is that number concentrations of individual microorganism types can be directly measured as a function of time. The most commonly observed species (2–10 µm) at the KNP site during this experiment were all fungal spores: *Cladosporium* spp., *Ganoderma* spp., basidiospores, and ascospores. Figure 2 shows a comparison of these species (with *Ganoderma* included in the Other category) alongside the size-resolved image plots of each fluorescence channel from the two real-time fluorescence instruments. The correlation of total biological particle concentration (Sporewatch) with WIBS and UV-APS may be more readily seen by comparing integrated number concentrations, however, as shown in Fig. 5. $N_{F,c}$ determined by WIBS FL2, FL3 and UV-APS, respectively, each show similar periods of high and low concentrations (Fig. 5b), though each channel is plotted with a different y-scale multiplier. This suggests that, despite the differing lists of fluorophores accessible to each channel, the groups of microorganisms selected are similar. The differing magnitude to the numbers, however, suggests that individual particles in each group possessing lower fluorescence emission are likely to be under-counted by the measurements and that the sensitivity of the detection scheme is important. The rise and fall of the Sporewatch peaks at similar time periods of the FL2, FL3, and UV-APS $N_{F,c}$ suggests a good qualitative comparison between the techniques and that these channels of the real-time fluorescence instruments are indeed successful in detecting biological aerosols such as these fungal spores.

In contrast to the qualitative similarity of the temporal trends of the WIBS FL2, FL3, and UV-APS numbers with the spore concentrations, the WIBS FL1 numbers bear little temporal similarity (Fig. 5a). $N_{F,c}$ from FL1 is influenced heavily by particles with $D < 2$ µm, which is collected less efficiently by the Sporewatch impactor. Thus the

ACPD
14, 3875–3915, 2014

population of particles detected by FL1 is largely separate than that of the particles observed by the paired Sporewatch/microscopy technique. These could be single or agglomerated bacteria particles that would be expected to fluoresce after excitation by 280 nm light of the FL1 channel. Though bacteria were not counted directly by the Sporewatch technique and cannot be determined directly by the UV-APS or WIBS, the number of fluorescent particles 1–2 µm in the WIBS FL1 channel is approx. 10^5 m^{-3}, which is an order of magnitude higher than $\sim 10^4$ m^{-3} commonly estimated as the concentration of bacteria present over vegetated surfaces (Després et al., 2012; Burrows et al., 2009b; Bauer et al., 2002). Thus, it is likely that bacteria were detected by this channel, but that these cannot explain all particles measured by this FL1. Sea spray enriched in sub-micron organic material, including proteins and other biological degradation products (Prather et al., 2013), can coat larger particles and may account for some of the FL1 particles and fluorescent coatings on particles observed via fluorescent microscopy. Additionally, the discrepancy between FL1 and Sporewatch number concentrations could be a result of hyaline particles not easily seen or counted using microscopy, but which could still fluoresce. This is less likely, however, because the process of fluorescent excitation is limited to particles that absorb, and so an individual particle in this hypothetical scenario would be expected to absorb strongly at 280 nm, but not so for visible (> 390 nm) identification. It is also unlikely that such biological particles would coincidentally fluoresce after 280 nm excitation, but not fluoresce with 355–370 nm excitation at the same time as being missed by visual counting. Lastly, it is possible that the FL1 channel counts a much higher number of non-biological particles that reduce the correlation with spore concentrations. These particles could be certain types of absorbing brown carbon secondary organic aerosol (Lee et al., 2013; Bones et al., 2010; Gabey et al., 2013) or soot particles (Panne et al., 2000; Lewitzka and Niessner, 1995), each expected to peak in number at sizes < 2 µm.

A quantitative view of the same correlations is shown in Fig. 6; $N_{F,c}$ from each channel plotted against a subset of the Sporewatch number (all classes except *Cladosporium*). In this case, the correlation of $N_{F,c}$ from the UV-APS is the highest with the spore

ACPD
14, 3875–3915, 2014

numbers (R^2 0.71), compared with R^2 of 0.05, 0.29, and 0.38 for WIBS FL1, FL2, and FL3 channels, respectively. In each comparison, however, the spore numbers are shown to undercount the real-time fluorescence measured numbers by factors of 3 to 14 (see Fig. 6). This is likely influenced heavily by the fact that the Sporewatch does not efficiently collect particles with $D < 2\,\mu m$, a size range that contain significant particle numbers measured by several of the fluorescence channels (Fig. 3). This is unlikely to be the only cause of the scaling factor, however, because the UV-APS did not show significant fluorescent particles in this size range, but still under-counted spores by a factor of 3. As a result, it could indicate that other fluorescent bioparticles (e.g. bacteria) or non-biological particles in the same size range can be associated with the same air masses, and thus would increase $N_{F,c}$ but not the contemporaneous spore numbers.

To highlight the similarity of each of the measurements styles, Fig. 7 shows diurnal (24 h) plots of spores observed (Fig. 7a) and of each fluorescence channel (Fig. 7b–e). Each measurement shows an increase in biological or fluorescent number concentration during the night and early morning hours (approx. 02:00–06:00 LT), with daily minima occurring in the mid-afternoon (approx. 15:00 LT). Figure 7 also shows the corresponding diurnal trend in relative humidity, which peaks at similar hours. This is consistent with commonly observed trends that many bioparticle classes correlate strongly with RH and peak at night (e.g. Toprak and Schnaiter, 2013; Schumacher et al., 2013; Huffman et al., 2012; Hirst, 1953; Rockett and Kramer, 1974). The UV-APS and WIBS FL3 channels each show mono-modal size distributions peaking at 3–4 µm through the night, while the FL2 channel shows a bio-modal distribution peaking at approx. 1 µm and 3–4 µm in size. These diurnal trends are reflected strongly by the concentrations of basidiospores and even more so by ascospores. Based on the observations via optical microscopy, the larger species (D ~3–4 µm) identified by the real-time fluorescence techniques are likely to be basidiospores and *Ganoderma* spp., while the smaller mode (D approx. 1 µm) observed for the FL2 channel may be comprised of ascospores. However, the identity of the smaller fluorescent particles is more uncertain, because the particles are relatively unidentifiably via optical microscopy because

ACPD
14, 3875–3915, 2014

of insufficient magnification. Huffman et al. (2012) argue, using diurnal measurements and comparison with previous literature reports, that $N_{F,c}$ from UV-APS observations in the Amazon rainforest are most likely to be a mixture of ascospores and basidiospores. Though measurements were conducted in a very different ecosystem, the conclusions here are consistent with earlier suggestions that UV-LIF measurements are particularly well suited to the detection of these bioparticle classes. Further, Manninen et al. (2014) present multi-year Sporewatch measurements in Hyytiälä, Finland and show that late summer (August and September) in N. Europe are peak seasons for many spores, including several groups of ascospores and basidiospores. Comparing with long-term UV-APS measurements reported by Schumacher et al. (2013), Manninen et al. (2014) suggest these classes of spores peak on a similar yearly cycle as the UV-APS $N_{F,c}$, and thus the August measurement period in this study coincides with a period of the year consistent with high fungal spore concentrations. Further, the fungal spore concentrations reported by Manninen et al. of $1–10 \times 10^4\ m^{-3}$ ($1–10 \times 10^{-2}\ cm^{-3}$) are within an order of magnitude of Sporewatch numbers reported here of $0.1–1 \times 10^{-2}\ cm^{-3}$.

In contrast to the diurnal trend of the ascospores and basidiospores, the Other category shows relatively flat diurnal profile, and the concentration of *Cladosporium* spp. spores shows a relative increase during the middle of the afternoon (peaking approx. 14:00). This temporal pattern for *Cladosporium* is expected and has been reported frequently. It is usually considered to be a dry weather spore whose concentration increases during warm periods of low relative humidity (De Groot, 1968; Oliveira et al., 2009). The interesting observation here is that the real-time fluorescence methods are relatively insensitive to the increases in *Cladosporium* spore concentration. Correlation plots of each fluorescence channel with *Cladosporium* spores show no qualitative pattern, with R^2 values < 0.006 in all cases. The reason for the relative insensitivity of these techniques to *Cladosporium* is unknown, but may relate to the dark-skinned (i.e. absorbing) nature of these spores preventing impinging photons from penetrating exterior pigments to excite fluorescence from internal fluorophores (Bell-Pedersen et al., 1996).

ACPD
14, 3875–3915, 2014

Diurnal patterns for additional meteorological measurements (e.g. air temperature, solar radiation, atmospheric pressure, and wind speed) observed during the entire measurement period are shown in Fig. S4. A consistent diurnal cycle was observed for RH with night time periods (campaign max 98 %) reaching higher values than during the day (campaign min 38 %). Minimum and maximum air temperatures recorded during the campaign were 4 °C and 26 °C, respectively, with a campaign average of 15 °C. Generally calm weather conditions, with several short periods of rain, were encountered throughout the entire campaign. This general pattern was reflected meteorologically by the lack of observable diurnal patterns for atmospheric pressure and also by low wind speeds.

3.4 Marine particle influence

Fluorescence microscopy images of size-resolved MOUDI stages collected during the study qualitatively show the presence of spores and other biological particles. The particles in the size range > 2 µm observed by the fluorescent microscopy technique to have the highest fluorescence were identified morphologically as PBAP. Many of the strongly fluorescent PBAP also demonstrated a clear cell wall fluorescence which suggests that it is not the cytosol or cellular metabolites such as NAD(P)H or riboflavin, but structural components of the cell wall that dominate the emission (Pöhlker et al., 2012, 2013). Many of the fluorescent PBAP also demonstrated fungal spore- like morphologies. Also frequently observed, however, were cubic particles that appear morphologically similar to NaCl (Fig. 8), and needle-like particles consistent with structures of crystals such as $CaSO_4$. No elemental analysis was possible on these particle agglomerates for confirmation, however. The observations of these inorganic-appearing particles suggest the influence of marine air containing sea salt. Of further interest is the appearance of bioparticles attached to the cubic salt-like particles, in which cases the bioparticle typically fluoresces strongly while the sea salt-like crystals do not. The number concentration of bioparticles and sea salt in the coarse particle mode make the agglomeration of these particles while airborne statistically unlikely. Thus, we sug-

ACPD
14, 3875–3915, 2014

gest that the bioparticle-salt agglomerates were likely emitted by marine sources and transported approx. 20 km from the ocean west of Ireland (Kenny and Jennings, 1998; Aller et al., 2005).

4 Conclusions

The study shows the measurement capabilities of the WIBS-4 and UV-APS to detect biological particles in a rural, ambient location and is the first to compare these two commercial sensors. Information revealed by each instrument is qualitatively similar, but key differences are apparent. Total coarse particle concentration ($N_{T,c}$) was shown to correlate well between the two instruments, and size distributions of total particles were similar. The UV-APS sizing measurement (aerodynamic diameter) showed more resolved distributions than did the WIBS-4 (optical diameter). This is likely a function of the physical properties of the particle sizing schemes in each instrument, and has been suggested previously. The minimum particle size detected by the WIBS-4, however, is related to the trigger threshold selected by the operator.

Concentrations of fluorescent particles observed during the measurement period by both instruments show regular, diurnal fluctuations that are qualitatively similar to each other. Differences in excitation/emission wavelength result in different particle populations observed, however. The UV-APS (λ_{ex} 355 nm) and WIBS FL3 channel (λ_{ex} 370 nm) correlate strongly, suggesting that the relative proximity of the excitation wavelengths allows each of these channels to excite similar fluorophores within interrogated particles. The UV-APS and WIBS FL3 channel show fluorescent particles dominated by a mode peaking at approx. 3 µm, with additional presence of a mode at approx. 1 µm present in FL3. The UV-APS $N_{F,c}$ was lower than FL3 $N_{F,c}$ by a factor of approx. 2.4, however, suggesting that the UV-APS particle detection sensitivity was relatively poor.

The WIBS FL2 channel showed a consistently bi-modal distribution comprised of 1 and µm modes and qualitatively appears to be a combination of modes present in the FL1 and FL3 channels. The WIBS FL2, FL3, and UV-APS particle numbers correlated

ACPD
14, 3875–3915, 2014

well in time and number with spore numbers collected via Sporewatch impactor and enumerated via optical microscopy. Each showed a diurnal peak in the early morning, with daily minima in the mid afternoon.

The WIBS FL1 channel, however, showed very different patterns. FL1 showed a relatively consistent diurnal pattern and a multi-modal size distribution with the highest concentration of fluorescent particles observed by any channel, but with the poorest correlation with spore numbers. This arises partially, because $N_{F,c}$ from FL1 was summed of particles with $D > 1$ µm, whereas the Sporewatch impaction technique is relatively inefficient at collecting particles < 2 µm. The smaller particles that escape Sporewatch detection, but that are recorded by the FL1 channel (λ_{ex} 270 nm) may include bacterial cells and protein-enriched coatings from sea spray origin. However, the discrepancy could also indicate the detection of non-biological particles such as certain absorbing SOA or soot into the FL1 particle number. It is thus clear from these observations that the multiple channels of fluorescent information delivered by the WIBS provide an advantage over the single fluorescence channel of the UV-APS. The qualitative similarity of diurnal patterns and of the UV-APS with WIBS FL3 channels highlights the utility of the UV-APS to detect the overall trends of fluorescent biological particles, however.

Comparisons between the real-time fluorescence instruments and the Sporewatch/microscopy technique reveal that the most likely species of airborne microorganism ($D > 2$ µm) present in Killarney National Park during the measurement period were spores, including basidiospores, ascospores, *Ganoderma* spp., and *Cladosporium* spp. The correlation of total spore concentration with the WIBS FL2, FL3, and UV-APS $N_{F,c}$ was high. However, *Cladosporium* spores correlated extremely poorly with all fluorescent measurements, suggesting that dark-walled cell walls may inhibit real-time fluorescence detection. Despite the presence of the spores observed, the microscopy results cannot rule out the possible contribution of soil bacteria such as actinobacteria and streptomycetes in the size range 1–2 µm that is not efficiently collected by the Sporewatch. These commonly airborne PBAP classes could also contribute to $N_{F,c}$ and reduce correlation with Sporewatch number.

ACPD
14, 3875–3915, 2014

The results of this study show that both WIBS and UV-APS techniques are capable of providing real-time information about biological aerosol particles, and that they can relate the major temporal trends of airborne fungal spores. Significant uncertainties still remain in the interpretation of the data from these instruments, and follow-up studies (e.g. systematic comparisons of the instruments in a controlled laboratory setting) will be necessary to inform further studies and analysis. For example, further work will be required to understand the nature of the poor correlation between spore concentration and WIBS FL1 number. Additional follow-up work will also be necessary to understand WIBS triggering thresholds to best characterize both fluorescent and non-fluorescent aerosol in field environments with unknown aerosol. These data show that the instruments performed well in a relatively clean, rural national park in western Ireland, but operational considerations will likely be different at sites more heavily influenced by anthropogenic aerosol sources. On the other hand UV-APS detected few of the smaller bacterial PBAP because of its single excitation wavelength. Measurements such as those presented here may provide direct inputs for the improvement of global models investigating the role of PBAP as IN or other cloud nuclei.

Relatively few estimates of PBAP concentrations exist, and the present study provides measured concentrations in a rural European environment. Further, the comparison of real-time fluorescence techniques capable of detecting fluorescent biological particles at high time and size resolution are supported by good correlations with direct observations of particles using optical microscopy (bright-field and fluorescence). These data support the idea that real-time fluorescence techniques can significantly improve time resolution and analysis time of traditional PBAP identification, which can be very laborious, time-consuming, and costly. Spore concentrations were observed on the order of $1–10 \times 10^4\ m^{-3}$, which is consistent with previous estimates (e.g. Després et al., 2012; Manninen et al., 2014; Elbert et al., 2007). Bacteria concentrations were not directly measured by these techniques, but the number of 1–2 µm particles in the WIBS FL1 channel is on the order of $10^5\ m^{-3}$, which could easily encompass the $\sim 10^4\ m^{-3}$ of bacteria commonly estimated to be present as a continental background

ACPD
14, 3875–3915, 2014

concentration (Després et al., 2012; Burrows et al., 2009b; Bauer et al., 2002). Observations that spore and FBAP concentrations cycle on a daily basis with RH and inversely with temperature are consistent with many previous reports that suggest many classes of fungal spores utilize periods of high humidity for active release (Elbert et al., 2007; Pringle et al., 2005; Jones and Harrison, 2004). Lastly, fluorescent microscopy images of sea salt-like particles agglomerated with biological cells suggests that air at the site was influenced by marine air and that the ocean provides one source for airborne biological material.

Supplementary material related to this article is available online at http://www.atmos-chem-phys-discuss.net/14/3875/2014/acpd-14-3875-2014-supplement.pdf.

Acknowledgements. The authors acknowledge the National Parks and Wildlife Service of Ireland for providing a sampling location in Killarney National Park with a suitable power supply. This work was financially supported by the Irish EPA BioCheA 2007 CCRP Project 4.4.6 and STRIVE Doctoral training program (2008-PhD-AQ-2). Financial support for J. A. Huffman, C. Pöhlker, and U. Pöschl was from the Max Planck Society, the Max Planck Graduate Center with the Johannes Gutenberg-Universität Mainz (MPGC), and the LEC Geocycles Mainz. J. A. Huffman acknowledges internal faculty funding from the University of Denver. The authors also acknowledge: J. Schneider and S. Borrmann (MPIC Particle Chemistry) for providing a UV-APS instrument; Eoin McGillicuddy, Ian O'Connor and Arnaud Allanic for help with the mobile laboratory and help transporting equipment. P. Kaye, W. Stanley are acknowledged for their technical support provided to project BioChea while David Dodd is acknowledged for his support of project BioChea.

ACPD
14, 3875–3915, 2014

References

Aller, J. Y., Kuznetsova, M. R., Jahns, C. J., and Kemp, P. F.: The sea surface microlayer as a source of viral and bacterial enrichment in marine aerosols, J. Aerosol Sci., 36, 801–812, doi:10.1016/j.jaerosci.2004.10.012, 2005.

Bauer, H., Kasper-Giebl, A., Löflund, M., Giebl, H., Hitzenberger, R., Zibuschka, F., and Puxbaum, H.: The contribution of bacteria and fungal spores to the organic carbon content of cloud water, precipitation and aerosols, Atmos. Res., 64, 109–119, 2002.

Bell-Pedersen, D., Garceau, N., and Loros, J. J.: Circadian rhythms in fungi, J. Genet., 75, 387–401, 1996.

Bones, D. L., Henricksen, D. K., Mang, S. A., Gonsior, M., Bateman, A. P., Nguyen, T. B., Cooper, W. J., and Nizkorodov, S. A.: Appearance of strong absorbers and fluorophores in limonene-O-3 secondary organic aerosol due to NH_4^+-mediated chemical aging over long time scales, J. Geophys. Res.-Atmos., 115, doi:10.1029/2009jd012864, 2010.

Brosseau, L. M., Vesley, D., Rice, N., Goodell, K., Nellis, M., and Hairston, P.: Differences in detected fluorescence among several bacterial species measured with a direct-reading particle sizer and fluorescence detector, Aerosol Sci. Tech., 32, 545–558, 2000.

Burrows, S. M., Butler, T., Jöckel, P., Tost, H., Kerkweg, A., Pöschl, U., and Lawrence, M. G.: Bacteria in the global atmosphere – Part 2: Modeling of emissions and transport between different ecosystems, Atmos. Chem. Phys., 9, 9281–9297, doi:10.5194/acp-9-9281-2009, 2009a.

Burrows, S. M., Elbert, W., Lawrence, M. G., and Pöschl, U.: Bacteria in the global atmosphere – Part 1: Review and synthesis of literature data for different ecosystems, Atmos. Chem. Phys., 9, 9263–9280, doi:10.5194/acp-9-9263-2009, 2009b.

Caruana, D. J.: Detection and analysis of airborne particles of biological origin: present and future, Analyst, 136, 4641–4652, doi:10.1039/c1an15506g, 2011.

Christner, B. C., Morris, C. E., Foreman, C. M., Cai, R. M., and Sands, D. C.: Ubiquity of biological ice nucleators in snowfall, Science, 319, 1214–1214, doi:10.1126/science.1149757, 2008.

De Groot, R. C.: Diurnal cycles of airborne spores produced by forest fungi, Phytopathology, 58, 1223–1229, 1968.

DeLeon-Rodriguez, N., Lathem, T. L., Rodriguez-R, L. M., Barazesh, J. M., Anderson, B. E., Beyersdorf, A. J., Ziemba, L. D., Bergin, M., Nenes, A., and Konstantinidis, K. T.: Mi-

ACPD
14, 3875–3915, 2014

crobiome of the upper troposphere: species composition and prevalence, effects of tropical storms, and atmospheric implications, P. Natl. Acad. Sci. USA, 110, 2575–2580, doi:10.1073/pnas.1212089110, 2013.

Després, V. R., Huffman, J. A., Burrows, S. M., Hoose, C., Safatov, A. S., Buryak, G. A., Fröhlich-Nowoisky, J., Elbert, W., Andreae, M. O., Pöschl, U., and Jaenicke, R.: Primary biological aerosol particles in the atmosphere: a review, Tellus B, 64, 15598, doi:10.3402/tellusb.v64i0.15598, 2012.

Diehl, K., Quick, C., Matthias-Maser, S., Mitra, S. K., and Jaenicke, R.: The ice nucleating ability of pollen – Part I: Laboratory studies in deposition and condensation freezing modes, Atmos. Res., 58, 75–87, 2001.

Elbert, W., Taylor, P. E., Andreae, M. O., and Pöschl, U.: Contribution of fungi to primary biogenic aerosols in the atmosphere: wet and dry discharged spores, carbohydrates, and inorganic ions, Atmos. Chem. Phys., 7, 4569–4588, doi:10.5194/acp-7-4569-2007, 2007.

Eng, J., Lynch, R. M., and Balaban, R. S.: Nicotinamide adenine dinucleotide fluorescence spectroscopy and imaging of isolated cardiac myocytes, Biophys. J., 55, 621–630, 1989.

Eversole, J. D., Hardgrove, J. J., Cary, W. K., Choulas, D. P., and Seaver, M.: Continuous, rapid biological aerosol detection with the use of UV fluorescence: outdoor test results, Field Anal. Chem. Tech., 3, 249–259, 1999.

Foot, V. E., Kaye, P. H., Stanley, W. R., Barrington, S. J., Gallagher, M., and Gabey, A.: Low-cost real-time multi-parameter bio-aerosol sensors, Proceedings of the SPIE – The International Society for Optical Engineering, 7116, 711601, doi:10.1117/12.800226, 2008.

Fröhlich-Nowoisky, J., Pickersgill, D. A., Despés, R. V., and Pöschl, U.: High diversity of fungi in air particulate matter, P. Natl. Acad. Sci. USA, 106, 12814–12819, doi:10.1073/pnas.0811003106, 2009.

Fröhlich-Nowoisky, J., Burrows, S. M., Xie, Z., Engling, G., Solomon, P. A., Fraser, M. P., Mayol-Bracero, O. L., Artaxo, P., Begerow, D., Conrad, R., Andreae, M. O., Després, V. R., and Pöschl, U.: Biogeography in the air: fungal diversity over land and oceans, Biogeosciences, 9, 1125–1136, doi:10.5194/bg-9-1125-2012, 2012.

Gabey, A. M., Gallagher, M. W., Whitehead, J., Dorsey, J. R., Kaye, P. H., and Stanley, W. R.: Measurements and comparison of primary biological aerosol above and below a tropical forest canopy using a dual channel fluorescence spectrometer, Atmos. Chem. Phys., 10, 4453–4466, doi:10.5194/acp-10-4453-2010, 2010.

ACPD
14, 3875–3915, 2014

Gabey, A. M., Stanley, W. R., Gallagher, M. W., and Kaye, P. H.: The fluorescence properties of aerosol larger than 0.8 µm in urban and tropical rainforest locations, Atmos. Chem. Phys., 11, 5491–5504, doi:10.5194/acp-11-5491-2011, 2011.

Gabey, A. M., Vaitilingom, M., Freney, E., Boulon, J., Sellegri, K., Gallagher, M. W., Crawford, I. P., Robinson, N. H., Stanley, W. R., and Kaye, P. H.: Observations of fluorescent and biological aerosol at a high-altitude site in central France, Atmos. Chem. Phys., 13, 7415–7428, doi:10.5194/acp-13-7415-2013, 2013.

Haga, D. I., Iannone, R., Wheeler, M. J., Mason, R., Polishchuk, E. A., Fetch, T., Jr., van der Kamp, B. J., McKendry, I. G., and Bertram, A. K.: Ice nucleation properties of rust and bunt fungal spores and their transport to high altitudes, where they can cause heterogeneous freezing, J. Geophys. Res.-Atmos., 118, 7260–7272, doi:10.1002/jgrd.50556, 2013.

Hairston, P. P., Ho, J., and Quant, F. R.: Design of an instrument for real-time detection of bioaerosols using simultaneous measurement of particle aerodynamic size and intrinsic fluorescence, J. Aerosol Sci., 28, 471–482, 1997.

Harrison, D. E. and Chance, B.: Fluorimetric technique for monitoring changes in level of reduced nicotinamide nucleotides in continuous cultures of microorganisms, Appl. Microbiol., 19, 446–450, 1970.

Heald, C. L. and Spracklen, D. V.: Atmospheric budget of primary biological aerosol particles from fungal spores, Geophys. Res. Lett., 36, L09806, doi:10.1029/2009gl037493, 2009.

Healy, D. A., O'Connor, D. J., Burke, A. M., and Sodeau, J. R.: A laboratory assessment of the Waveband Integrated Bioaerosol Sensor (WIBS-4) using individual samples of pollen and fungal spore material, Atmos. Environ., 60, 534–543, doi:10.1016/j.atmosenv.2012.06.052, 2012a.

Healy, D. A., O'Connor, D. J., and Sodeau, J. R.: Measurement of the particle counting efficiency of the "Waveband Integrated Bioaerosol Sensor" model number 4 (WIBS-4), J. Aerosol Sci., 47, 94–99, doi:10.1016/j.jaerosci.2012.01.003, 2012b.

Hill, S. C., Pinnick, R. G., Niles, S., Fell, N. F., Pan, Y. L., Bottiger, J., Bronk, B. V., Holler, S., and Chang, R. K.: Fluorescence from airborne microparticles: dependence on size, concentration of fluorophores, and illumination intensity, Appl. Optics, 40, 3005–3013, 2001.

Hirst, J. M.: An automatic volumetric spore trap, Ann. Appl. Biol., 39, 257–265, doi:10.1111/j.1744-7348.1952.tb00904.x, 1952.

ACPD
14, 3875–3915, 2014

Hirst, J. M.: Changes in atmospheric spore content: diurnal periodicity and the effects of weather, T. Brit. Mycol. Soc., 36, 375–393, IN378, doi:10.1016/s0007-1536(53)80034-3, 1953.

Ho, J.: Future of biological aerosol detection, Anal. Chim. Acta, 457, 125–148, 2002.

Hoose, C., Kristjansson, J. E., and Burrows, S. M.: How important is biological ice nucleation in clouds on a global scale?, Environ. Res. Lett., 5, 024009, doi:10.1088/1748-9326/5/2/024009, 2010.

Huffman, J. A., Treutlein, B., and Pöschl, U.: Fluorescent biological aerosol particle concentrations and size distributions measured with an Ultraviolet Aerodynamic Particle Sizer (UV-APS) in Central Europe, Atmos. Chem. Phys., 10, 3215–3233, doi:10.5194/acp-10-3215-2010, 2010.

Huffman, J. A., Sinha, B., Garland, R. M., Snee-Pollmann, A., Gunthe, S. S., Artaxo, P., Martin, S. T., Andreae, M. O., and Pöschl, U.: Size distributions and temporal variations of biological aerosol particles in the Amazon rainforest characterized by microscopy and real-time UV-APS fluorescence techniques during AMAZE-08, Atmos. Chem. Phys., 12, 11997–12019, doi:10.5194/acp-12-11997-2012, 2012.

Huffman, J. A., Prenni, A. J., DeMott, P. J., Pöhlker, C., Mason, R. H., Robinson, N. H., Fröhlich-Nowoisky, J., Tobo, Y., Després, V. R., Garcia, E., Gochis, D. J., Harris, E., Müller-Germann, I., Ruzene, C., Schmer, B., Sinha, B., Day, D. A., Andreae, M. O., Jimenez, J. L., Gallagher, M., Kreidenweis, S. M., Bertram, A. K., and Pöschl, U.: High concentrations of biological aerosol particles and ice nuclei during and after rain, Atmos. Chem. Phys., 13, 6151–6164, doi:10.5194/acp-13-6151-2013, 2013.

Hummel, M., Vogel, H., Toprak, E., Schnaiter, M., Robinson, N. H., Gallagher, M., Huffman, J. A., Pöhlker, C., Pöschl, U., and Hoose, C.: Regional-scale simulations of fungal spore aerosols using an emission parameterization adapted to local measurements of fluorescent biological aerosol particles, Atmos. Chem. Phys., in preparation, 2014.

Jones, A. M. and Harrison, R. M.: The effects of meteorological factors on atmospheric bioaerosol concentrations – a review, Sci. Total Environ., 326, 151–180, doi:10.1016/j.scitotenv.2003.11.021, 2004.

Kaye, P. H., Stanley, W. R., Hirst, E., Foot, E. V., Baxter, K. L., and Barrington, S. J.: Single particle multichannel bio-aerosol fluorescence sensor, Opt. Express, 13, 3583–3593, 2005.

Kenny, C. M. and Jennings, S. G.: Background bioaerosol measurements at Mace Head, J. Aerosol Sci., 29, S779–S780, doi:10.1016/S0021-8502(98)90572-9, 1998.

ACPD
14, 3875–3915, 2014

Khattab, A. and Levetin, E.: Preliminary studies on the effect of the Burkard alternate orifice on airborne fungal spore concentrations., Aerobiologia, 24, 165–171, 2008.
Lacey, J. and Dutkiewicz, J.: Bioaerosols and occupational lung disease, J. Aerosol Sci., 25, 1371–1404, 1994.
Lacey, J. and Venette, J.: Outdoor air sampling techniques, in: Bioaerosols Handbook, edited by: Cox, C. S. and Wathes, C. M., Lewis Publishers, Boca Raton, FL, 407–471, 1995.
Lacey, M. E. and West, J. S.: The air spora: a manual for catching and identifying airborne biological particles, Springer, 2006.
Lee, H. J., Laskin, A., Laskin, J., and Nizkorodov, S. A.: Excitation–emission spectra and fluorescence quantum yields for fresh and aged biogenic secondary organic aerosols, Environ. Sci. Technol., 47, 5763–5770, doi:10.1021/es400644c, 2013.
Lewitzka, F. and Niessner, R.: Application of time-resolved fluorescence spectroscopy on the analysis of PAH-coated aerosols, Aerosol Sci. Tech., 23, 454–464, doi:10.1080/02786829508965328, 1995.
Li, J. K., Asali, E. C., and Humphrey, A. E.: Monitoring cell concentration and activity by multiple excitation flourometry, Biotechnol. Progr., 7, 21–27, 1991.
Madelin, T. M.: Fungal aerosols – a review, J. Aerosol Sci., 25, 1405–1412, doi:10.1016/0021-8502(94)90216-x, 1994.
Maki, L. R., Glyan, E. L., Chang-Chien, M. M., and Caldwell, D. R.: Ice nucleation induced by *Pseudomonas syringae*, Appl. Environ. Microb., 28, 456–459, 1974.
Manninen, H. E., Sihto-Nissilä, S.-L., Huffman, J. A., Bäck, J., Pessi, A.-M., Hiltunen, V., Aalto, P., Hidalgo, P. J., Hari, P., Saarto, A., Kulmala, M., and Petäjä, T.: Annual pattern of airborne pollen grains, fungal spores and particle mass in a boreal forest, Boreal Environ. Res., in review, 2014.
Marple, V. A., Rubow, K. L., and Behm, S. M.: A microorifice uniform deposit impactor (MOUDI) – description, calibration, and use, Aerosol Sci. Tech., 14, 434–446, doi:10.1080/02786829108959504, 1991.
Möhler, O., DeMott, P. J., Vali, G., and Levin, Z.: Microbiology and atmospheric processes: the role of biological particles in cloud physics, Biogeosciences, 4, 1059–1071, doi:10.5194/bg-4-1059-2007, 2007.
Morris, C. E., Georgakopoulos, D. G., and Sands, D. C.: Ice nucleation active bacteria and their potential role in precipitation, J. Phys. IV, 121, 87–103, doi:10.1051/jp4:2004121004, 2004.

ACPD
14, 3875–3915, 2014

Morris, C. E., Sands, D. C., Vinatzer, B. A., Glaux, C., Guilbaud, C., Buffiere, A., Yan, S., Dominguez, H., and Thompson, B. M.: The life history of the plant pathogen Pseudomonas syringae is linked to the water cycle, ISME J., 2, 321–334, 2008.

Morris, C. E., Sands, D. C., Glaux, C., Samsatly, J., Asaad, S., Moukahel, A. R., Gonçalves, F. L. T., and Bigg, E. K.: Urediospores of rust fungi are ice nucleation active at $> -10\ ^{\circ}C$ and harbor ice nucleation active bacteria, Atmos. Chem. Phys., 13, 4223–4233, doi:10.5194/acp-13-4223-2013, 2013.

Morris, C. E., Conen, F., Huffman, J. A., Phillips, V., Pöschl, U., and Sands, D. C.: Bio-precipitation: a feedback cycle linking Earth history, ecosystem dynamics and land use through biological ice nucleators in the atmosphere, Glob. Change Biol., 20, 341–351, doi:10.1111/gcb.12447, 2014.

O'Connor, D. J., Healy, D. A., and Sodeau, J. R.: The on-line detection of biological particle emissions from selected agricultural materials using the WIBS-4 (Waveband Integrated Bioaerosol Sensor) technique, Atmos. Environ., 80, 415–425, doi:10.1016/j.atmosenv.2013.07.051, 2013.

Oliveira, M., Ribeiro, H., Delgado, J., and Abreu, I.: The effects of meteorological factors on airborne fungal spore concentration in two areas differing in urbanisation level, Int. J. Biometeorol., 53, 61–73, doi:10.1007/s00484-008-0191-2, 2009.

Pan, Y. L., Pinnick, R. G., Hill, S. C., Rosen, J. M., and Chang, R. K.: Single-particle laser-induced-fluorescence spectra of biological and other organic-carbon aerosols in the atmosphere: measurements at New Haven, Connecticut, and Las Cruces, New Mexico, J. Geophys. Res.-Atmos., 112, 15, doi:10.1029/2007jd008741, 2007.

Pan, Y.-L., Hill, S. C., Pinnick, R. G., House, J. M., Flagan, R. C., and Chang, R. K.: Dual-excitation-wavelength fluorescence spectra and elastic scattering for differentiation of single airborne pollen and fungal particles, Atmos. Environ., 45, 1555–1563, doi:10.1016/j.atmosenv.2010.12.042, 2011.

Panne, U., Knöller, A., Kotzick, R., and Niessner, R.: On-line and in-situ detection of polycyclic aromatic hydrocarbons (PAH) on aerosols via thermodesorption and laser-induced fluorescence spectroscopy, Fresen. J. Anal. Chem., 366, 408–414, doi:10.1007/s002160050083, 2000.

Patel, N. J. and Bush, R. K.: Role of environmental allergens in rhinitis, Immunol. Allergy Clin., 20, 323–353, doi:10.1016/S0889-8561(05)70151-X, 2000.

ACPD
14, 3875–3915, 2014

Pinnick, R. G., Hill, S. C., Nachman, P., Pendleton, J. D., Fernandez, G. L., Mayo, M. W., and Bruno, J. G.: Fluorescence particle counter for detecting airborne bacteria and other biological particles, Aerosol Sci. Tech., 23, 653–664, 1995.

Pinnick, R. G., Hill, S. C., Pan, Y. L., and Chang, R. K.: Fluorescence spectra of atmospheric aerosol at Adelphi, Maryland, USA: measurement and classification of single particles containing organic carbon, Atmos. Environ., 38, 1657–1672, doi:10.1016/j.atmosenv.2003.11.017, 2004.

Pöhlker, C., Huffman, J. A., and Pöschl, U.: Autofluorescence of atmospheric bioaerosols – fluorescent biomolecules and potential interferences, Atmos. Meas. Tech., 5, 37–71, doi:10.5194/amt-5-37-2012, 2012.

Pöhlker, C., Huffman, J. A., Förster, J.-D., and Pöschl, U.: Autofluorescence of atmospheric bioaerosols: spectral fingerprints and taxonomic trends of pollen, Atmos. Meas. Tech., 6, 3369–3392, doi:10.5194/amt-6-3369-2013, 2013.

Pöschl, U.: Atmospheric aerosols: composition, transformation, climate and health effects, Angew. Chem. Int. Edit., 44, 7520–7540, doi:10.1002/anie.200501122, 2005.

Pöschl, U., Martin, S. T., Sinha, B., Chen, Q., Gunthe, S. S., Huffman, J. A., Borrmann, S., Farmer, D. K., Garland, R. M., Helas, G., Jimeney, J. L., King, S. M., Manzi, A., Mikhailov, E., Pauliquevis, T., Petters, M. D., Prenni, A. J., Roldin, P., Rose, D., Schneider, J., Su, H., Zorn, S. R., Artaxo, P., and Andreae, M. O.: Rainforest aerosols as biogenic nuclei of clouds and precipitation in the Amazon, Science, 329, 1513–1516, doi:10.1126/science.1191056, 2010.

Prather, K. A., Bertram, T. H., Grassian, V. H., Deane, G. B., Stokes, M. D., DeMott, P. J., Aluwihare, L. I., Palenik, B. P., Azam, F., Seinfeld, J. H., Moffet, R. C., Molina, M. J., Cappa, C. D., Geiger, F. M., Roberts, G. C., Russell, L. M., Ault, A. P., Baltrusaitis, J., Collins, D. B., Corrigan, C. E., Cuadra-Rodriguez, L. A., Ebben, C. J., Forestieri, S. D., Guasco, T. L., Hersey, S. P., Kim, M. J., Lambert, W. F., Modini, R. L., Mui, W., Pedler, B. E., Ruppel, M. J., Ryder, O. S., Schoepp, N. G., Sullivan, R. C., and Zhao, D.: Bringing the ocean into the laboratory to probe the chemical complexity of sea spray aerosol, P. Natl. Acad. Sci. USA, 110, 7550–7555, doi:10.1073/pnas.1300262110, 2013.

Prenni, A. J., Tobo, Y., Garcia, E., DeMott, P. J., Huffman, J. A., McCluskey, C. S., Kreidenweis, S. M., Prenni, J. E., Pöhlker, C., and Pöschl, U.: The impact of rain on ice nuclei populations at a forested site in Colorado, Geophys. Res. Lett., 40, 227–231, doi:10.1029/2012gl053953, 2013.

ACPD
14, 3875–3915, 2014

Pringle, A., Patek, S. N., Fischer, M., Stolze, J., and Money, N. P.: The captured launch of a ballistospore, Mycologia, 97, 866–871, doi:10.3852/mycologia.97.4.866, 2005.
Pummer, B. G., Bauer, H., Bernardi, J., Bleicher, S., and Grothe, H.: Suspendable macromolecules are responsible for ice nucleation activity of birch and conifer pollen, Atmos. Chem. Phys., 12, 2541–2550, doi:10.5194/acp-12-2541-2012, 2012.
Robinson, N. H., Allan, J. D., Huffman, J. A., Kaye, P. H., Foot, V. E., and Gallagher, M.: Cluster analysis of WIBS single-particle bioaerosol data, Atmos. Meas. Tech., 6, 337–347, doi:10.5194/amt-6-337-2013, 2013.
Rockett, T. R. and Kramer, C. L.: Periodicity and total spore production by lignicolous basidiomycetes, Mycologia, 66, 817–829, 1974.
Sands, D. C., Langhans, V. E., Scharen, A. L., and de Smet, G.: The association between bacteria and rain and possible resultant meteorological implications, Journal of the Hungarian Meteorological Service, 86, 148–152, 1982.
Schumacher, C. J., Pöhlker, C., Aalto, P., Hiltunen, V., Petäjä, T., Kulmala, M., Pöschl, U., and Huffman, J. A.: Seasonal cycles of fluorescent biological aerosol particles in boreal and semi-arid forests of Finland and Colorado, Atmos. Chem. Phys., 13, 11987–12001, doi:10.5194/acp-13-11987-2013, 2013.
Sesartic, A., Lohmann, U., and Storelvmo, T.: Modelling the impact of fungal spore ice nuclei on clouds and precipitation, Environ. Res. Lett., 8, 014029, doi:10.1088/1748-9326/8/1/014029, 2013.
Setlow, B. and Setlow, P.: Levels of oxidized and reduced pyridine nucleotides in dormant spores and during growth, sporulation, and spore germination of bacillus megaterium, J. Bacteriol., 129, 857–865, 1977.
Shiraiwa, M., Selzle, K., and Poeschl, U.: Hazardous components and health effects of atmospheric aerosol particles: reactive oxygen species, soot, polycyclic aromatic compounds and allergenic proteins, Free Radical Res., 46, 927–939, doi:10.3109/10715762.2012.663084, 2012.
Sivaprakasam, V., Huston, A. L., Scotto, C., and Eversole, J. D.: Multiple UV wavelength excitation and fluorescence of bioaerosols, Opt. Express, 12, 4457–4466, 2004.
Sivaprakasam, V., Lin, H.-B., Huston, A. L., and Eversole, J. D.: Spectral characterization of biological aerosol particles using two-wavelength excited laser-induced fluorescence and elastic scattering measurements, Opt. Express, 19, 6191–6208, 2011.

ACPD
14, 3875–3915, 2014

Stanley, W. R., Kaye, P. H., Foot, V. E., Barrington, S. J., Gallagher, M., and Gabey, A.: Continuous bioaerosol monitoring in a tropical environment using a UV fluorescence particle spectrometer, Atmos. Sci. Lett., 12, 195–199, doi:10.1002/asl.310, 2011.

Sterling, M., Rogers, C., and Levetin., E.: An evaluation of two methods used for microscopic analysis of airborne fungal spore concentrations from the Burkard Spore Trap., Aerobiologia, 15, 9–18, 1999.

Tanke, H. J., van Oostveldt, P., and van Duijn, P.: A parameter for the distribution of fluorophores in cells derived from measurements of inner filter effect and reabsorption phenomenon, Cytometry, 2, 359–369, doi:10.1002/cyto.990020602, 1982.

Toprak, E. and Schnaiter, M.: Fluorescent biological aerosol particles measured with the Waveband Integrated Bioaerosol Sensor WIBS-4: laboratory tests combined with a one year field study, Atmos. Chem. Phys., 13, 225–243, doi:10.5194/acp-13-225-2013, 2013.

Womack, A. M., Bohannan, B. J. M., and Green, J. L.: Biodiversity and biogeography of the atmosphere, Philos. T. R. Soc. B, 365, 3645–3653, doi:10.1098/rstb.2010.0283, 2010.

Xu, Z., Wu, Y., Shen, F., Chen, Q., Tan, M., and Yao, M.: Bioaerosol science, technology, and engineering: past, present, and future, Aerosol Sci. Tech., 45, 1337–1349, doi:10.1080/02786826.2011.593591, 2011.

ACPD
14, 3875–3915, 2014

Table 1. A comparison between instrumental parameters used during the study for the UV-APS and WIBS-4 techniques.

	UV-APS (TSI Model no. 3314)	WIBS (Univ. Hertfordshire Model no. 4)
Summary of measurement capabilities	particle size, intrinsic particle fluorescence (1 channel), particle side-scatter light intensity	particle size, intrinsic particle fluorescence (3 channels), particle asymmetry
Aerosol sample flow rate	1.0 L min^{-1}	0.23 L min^{-1}
Sampling Time	User-defined binning (5 min here)	Individual particle detection (post-binned to 5 min)
Sizing Method	Aerodynamic Diameter (D_a)	Optical Diameter (D_o)
Size resolution	52 channels selected	52 channels selected (only 45 used due to max D_o ~13 µm)
Particle Size Range	D_a: ~ 0.5 to ~ 20 µm	D_o: ~ 0.5 µm to ~ 13 µm
Excitation source	355 nm via UV laser (Nd:YAG)	280 nm and 370 nm via Xenon flash-tubes with blocking filters
Fluorescence	λ_{ex} = 355 nm λ_{em} = 420–580 nm	FL 1 λ_{ex} = 280 nm λ_{em} = 310–400 nm FL 2 λ_{ex} = 280 nm λ_{em} = 420–650 nm FL 3 λ_{ex} = 370 nm λ_{em} = 420–650 nm
Particle Asymmetry	n/a	A_F via side-scatter intensity in four quadrants (A_F = 0, sphere; $A_F \gg 0$, high aspect ratio fibre)

ACPD
14, 3875–3915, 2014

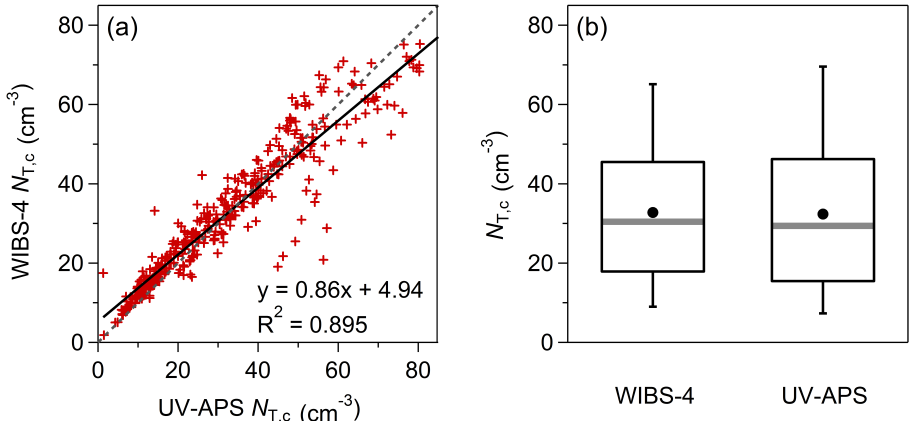

Fig. 1. Comparison of concentrations of total coarse particles ($D > 1\,\mu m$) over the entire ~ 1 month measurement period. Red symbols **(a)** show 5 min data points, and solid black line shows linear fit (not weighted). Dashed line is 1 : 1 line. Statistical summary of $N_{T,c}$ shown as box-whisker plots **(b)**. Black dots (mean), horizontal grey bar (median), boxes (25–75th percentile), vertical bars (5–9th percentile).

ACPD
14, 3875–3915, 2014

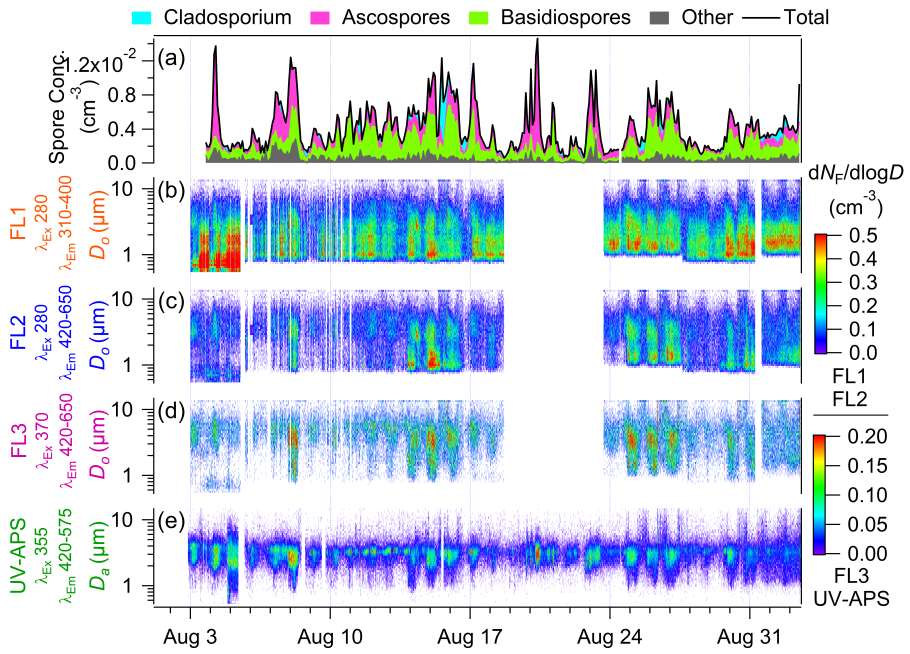

Fig. 2. Campaign overview time series. Selected biological particles identified by Sporewatch technique **(a)**. Size-resolved measurements of fluorescent particles as determined by: WIBS FL1 **(b)**, FL2 **(c)**, and FL3 **(d)** channels, and UV-APS **(e)**. Color scale for image plots **(b–e)** shown as dN_F/d log$D$ (cm^{-3}) on right and is separated into FL1, FL2 (upper scale) and FL3, UVAPS (lower scale). Data reported for both WIBS-4 and UV-APS as 5 min averages and for Sporewatch as 2 h averages.

ACPD
14, 3875–3915, 2014

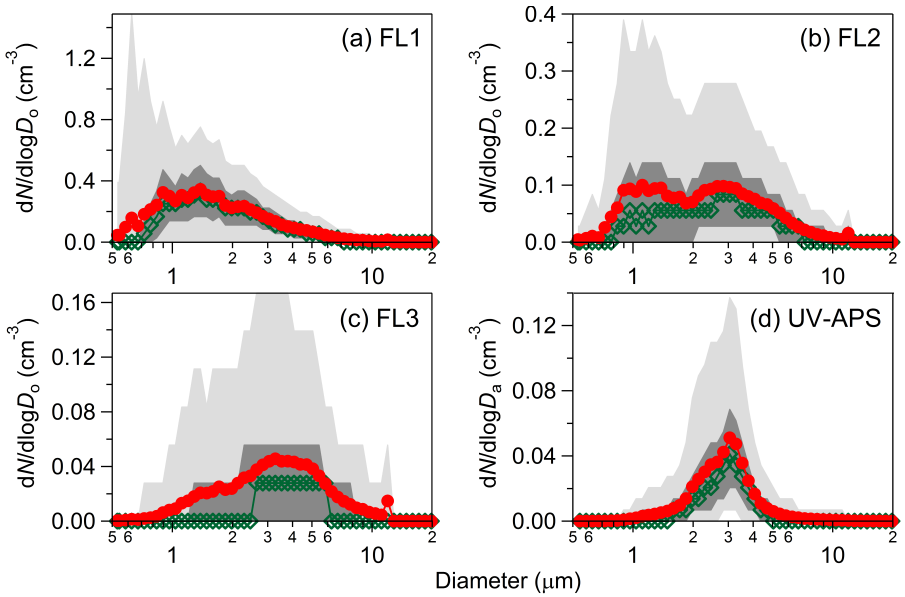

Fig. 3. Average FBAP number size distributions measured by WIBS-4 for **(a)** FL1, **(b)** FL2 **(c)** FL3 and **(d)** UV-APS for the entire sampling period. Red traces show mean values, green traces show median, dark gray areas show 25–75th percentile, and light gray areas show 5–95th percentiles. Vertical scacle is different in each panel.

ACPD
14, 3875–3915, 2014

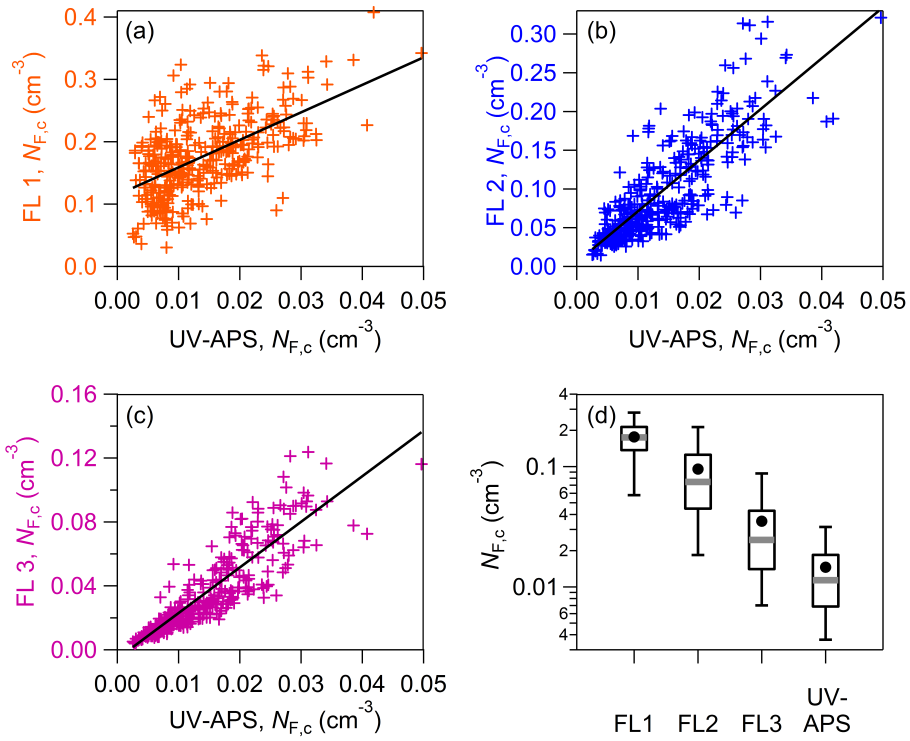

Fig. 4. Comparison of coarse (> 1 µm) fluorescent particle number ($N_{F,c}$) between individual WIBS channels and UV-APS shown for entire measurement period. Coloured crosses show individual 5 min data **(a–c)**, and black diagonal lines show un-weighted linear fits. Correlation coefficients are: FL1, R^2 0.34 **(a)**; FL2, R^2 0.68 **(b)**; FL3, R^2 0.78 **(c)**. Statistical overview of all data shown for each channel as box-whisker plots **(d)**; black dot mean, horizontal gray bar median, black box 25–75th percentile, vertical bars 5–95th percentiles. Vertical scales are different in each correlation plot **(a–c)**.

ACPD
14, 3875–3915, 2014

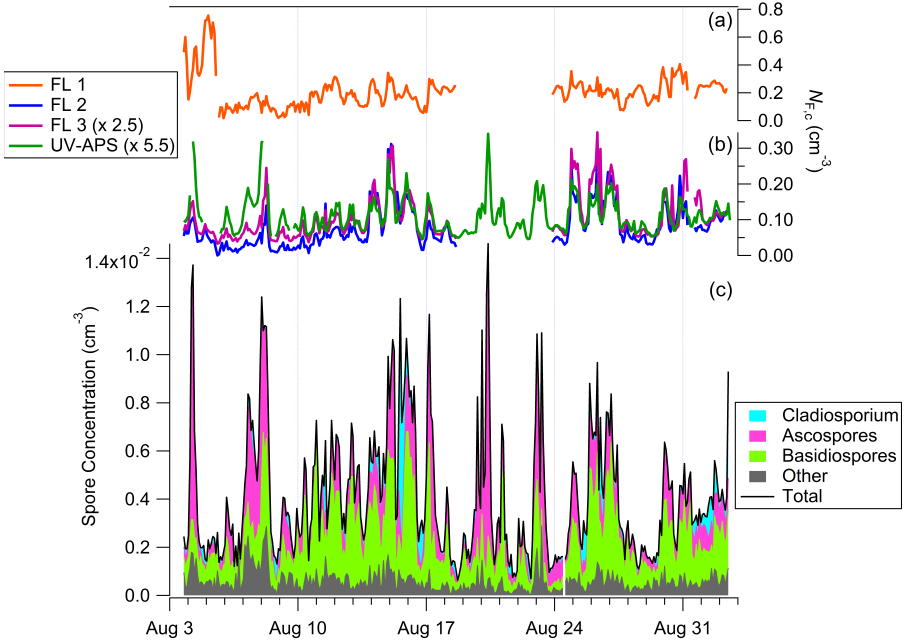

Fig. 5. Temporal trends observed for coarse fluorescent particles **(a–b)** and spores sampled by Sporewatch **(c)**. WIBS FL1 $N_{F,c}$ plotted alone **(a)**, WIBS FL2, FL3, and UV-APS $N_{F,c}$ traces plotted together **(b)**. Scaler value for FL3 and UV-APS traces shown in legend, showing that these traces have been multiplied by the value to show on one axis. All three vertical axes have different scales.

ACPD
14, 3875–3915, 2014

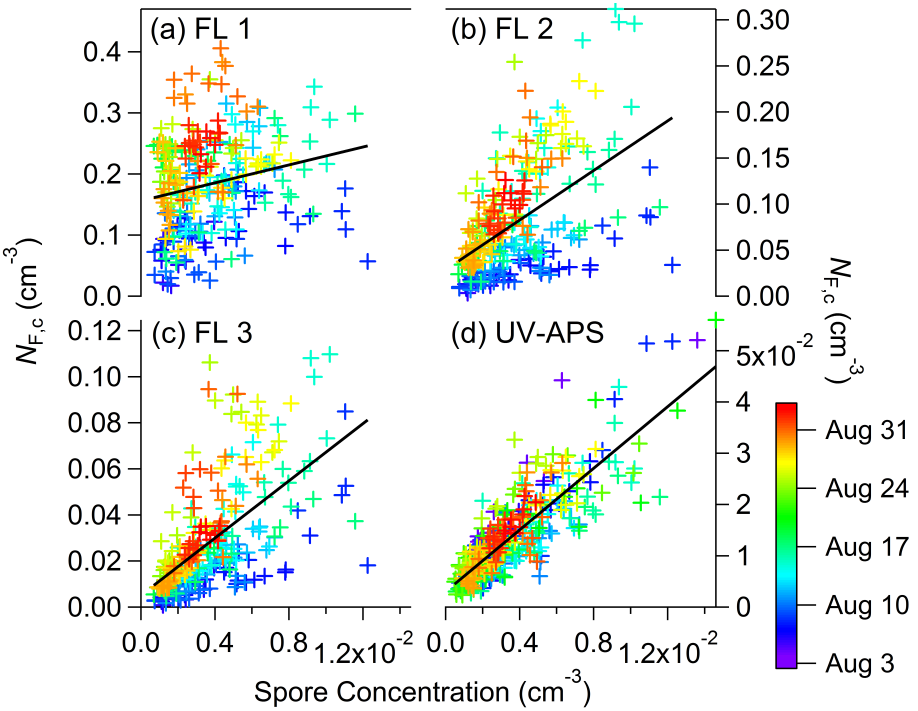

Fig. 6. Demonstrated relationship of $N_{F,C}$ determined by the real-time instruments vs. a sum of a subset of spores collected by the Sporewatch impactor. Spores here include: ascospores, basidiospores, and *Ganoderma* spp., which relate approx. 88 % of total spore concentration (remaining percentage *Cladosporium* spp.). Crosses represent 2 h measurement points, coloured by sampling date. Black lines represent un-weighted linear fits, with coefficients as follows: **(a)** FL1 (m = 7.67, R^2 = 0.052); **(b)** FL2 (m = 14.03, R^2 = 0.290); **(c)** FL3 (m = 6.47, R^2 = 0.380); **(d)** UV-APS (m = 3.00, R^2 = 0.710). All vertical axes have different scales.

ACPD
14, 3875–3915, 2014

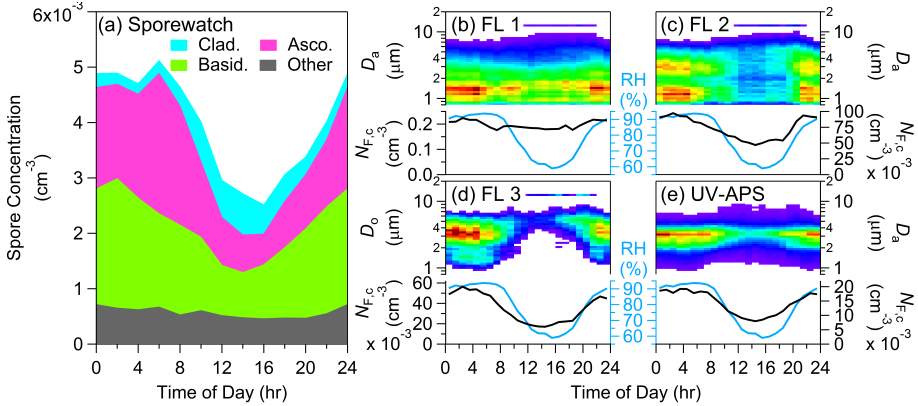

Fig. 7. Diurnal plots of number concentrations from Sporewatch **(a)** and real-time fluorescence instruments **(b–e)** as median values for entire sampling period. Upper panel of WIBS and UV-APS plots **(b–e)** show size-resolved image, with colour scale qualitatively similar to Fig. 2 (warmer colours, higher concentration). Lower panel of the same plots show integrated fluorescent particle number ($N_{F,c}$; $D > 1$ µm) as black trace and relative humidity as blue trace. Vertical scale on $N_{F,c}$ axes not consistent.

ACPD
14, 3875–3915, 2014

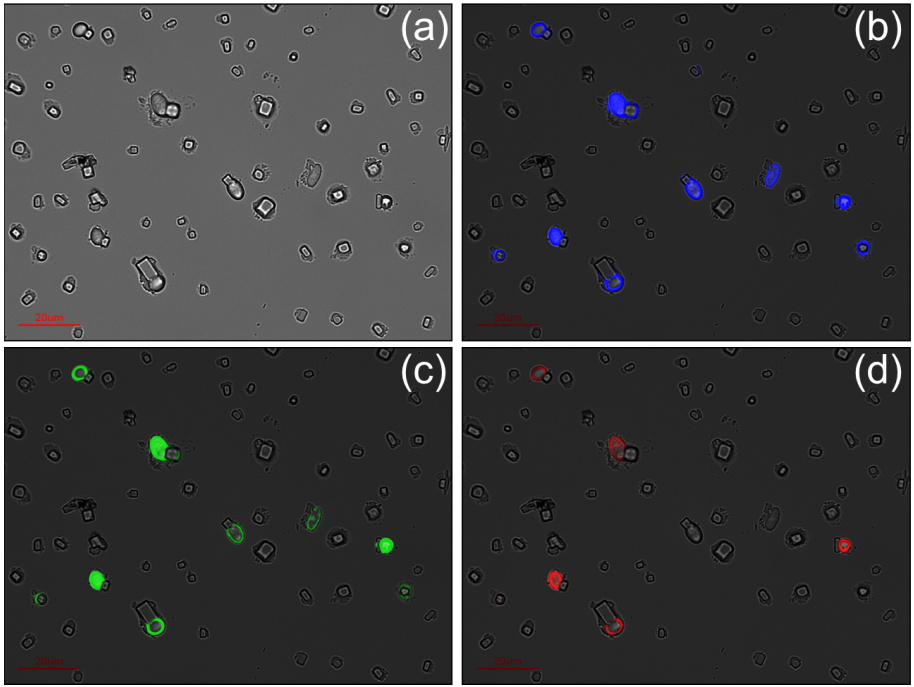

Fig. 8. Fluorescence microscopy images of ambient aerosols collected on MOUDI stage 5 (size range, D 1.0–1.8 µm) on 25 August, 03:00–07:00 LT. Illumination source: **(a)** bright field, **(b)** λ_{ex} = 340–380 nm, λ_{em} = 435–485, **(c)** λ_{ex} = 465–495 nm, λ_{em} = 510–560, **(d)** λ_{ex} = 540–580 nm, λ_{em} = 600–660. Magnification ×1000.

ACPD
14, 3875–3915, 2014